

# Canonical description of the new LHCb resonances

Pablo G. Ortega,<sup>1,\*</sup> Jorge Segovia,<sup>2,†</sup> David R. Entem,<sup>3,‡</sup> and Francisco Fernández<sup>3,§</sup>

<sup>1</sup>*Instituto de Física Corpuscular (IFIC),  
Centro Mixto CSIC-Universidad de Valencia,  
ES-46071 Valencia, Spain*

<sup>2</sup>*Physik-Department, Technische Universität München,  
James-Franck-Str. 1, 85748 Garching, Germany*

<sup>3</sup>*Grupo de Física Nuclear and Instituto Universitario de Física Fundamental y Matemáticas (IUFFyM),  
Universidad de Salamanca, E-37008 Salamanca, Spain*

(Dated: October 4, 2018)

The LHCb Collaboration has recently observed four  $J/\psi\phi$  structures called  $X(4140)$ ,  $X(4274)$ ,  $X(4500)$  and  $X(4700)$  in the  $B^+ \rightarrow J/\psi\phi K^+$  decays. We study them herein using a nonrelativistic constituent quark model in which the degrees of freedom are quark-antiquark and meson-meson components. The  $X(4140)$  resonance appears as a cusp in the  $J/\psi\phi$  channel due to the near coincidence of the  $D_s^\pm D_s^{*\mp}$  and  $J/\psi\phi$  mass thresholds. The remaining three  $X(4274)$ ,  $X(4500)$  and  $X(4700)$  appear as conventional charmonium states with quantum numbers  $3^3P_1$ ,  $4^3P_0$  and  $5^3P_0$ , respectively; and whose masses and widths are slightly modified due to their coupling with the corresponding closest meson-meson thresholds. A particular feature of our quark model is a lattice-based screened linear confining interaction that has been constrained in the light quark sector and usually produces higher excited heavy-quark states with lower masses than standard quark model predictions.

PACS numbers: 12.39.Pn, 14.40.Lb, 14.40.Rt

Keywords: Potential models, Charmed mesons, Exotic mesons

One of the basic properties of Quantum Chromodynamics (QCD) is its spectrum: the list of particles that are stable or at least sufficiently long-lived to be observed as resonances. The elementary constituents in QCD are quarks ( $q$ ), antiquarks ( $\bar{q}$ ), and gluons ( $g$ ), and QCD requires them to be confined into colour-singlet clusters called hadrons. The most stable hadrons are the clusters predicted by the quark model [1, 2], conventional mesons ( $q\bar{q}$ ), baryons ( $qqq$ ) and antibaryons ( $\bar{q}\bar{q}\bar{q}$ ), which have been the only states observed in experiments for around 30 years [3].

This simple picture is being challenged since 2003 with the discovery of almost two dozen charmonium- and bottomonium-like XYZ states that do not fit the naive quark-antiquark interpretation. Most of these states usually appear close to meson-meson thresholds and thus their dynamics can be strongly dictated by the nearby multi-quark channels. In fact, the discovery of the XYZ particles is opening the door to systematically explore higher Fock components of the meson wave function such as molecules, compact tetraquarks or diquark-antidiquark (diquarkonium) structures.

The  $X(4140)$ ,  $X(4274)$ ,  $X(4500)$  and  $X(4700)$  are some of the last XYZ states observed, this time, in the amplitude analysis of  $B^+ \rightarrow J/\psi\phi K^+$  decays performed by the LHCb Collaboration [4, 5]. The  $X(4140)$  was previously seen by CDF [6], D0 [7], CMS [8], Belle [9] and

BaBar [10] Collaborations; the rest:  $X(4274)$ ,  $X(4500)$  and  $X(4700)$  have been determined for the first time with the LHCb experiment.

Thanks to the large signal yield, the roughly uniform efficiency and the relatively low background across the entire  $J/\psi\phi$  mass range, the LHCb data [4, 5] offers the best sensitivity to date in order to probe the nature of the observed structures, but also to establish their quantum numbers. The quantum numbers of the  $X(4140)$  and  $X(4274)$  are determined to be  $J^{PC} = 1^{++}$  with statistical significance  $5.7\sigma$  and  $5.8\sigma$ , respectively. The  $X(4500)$  and  $X(4700)$  resonances have both  $J^{PC} = 0^{++}$  with statistical significance  $4.0\sigma$  and  $4.5\sigma$ , respectively.

The determination by the LHCb Collaboration of the  $J^{PC} = 1^{++}$  quantum numbers for the  $X(4140)$  and  $X(4274)$  resonances have had a big impact on their theoretical interpretations, ruling out most of the multi-quark models. Lebed-Polosa [11] predicted the  $X(4140)$  to be a  $1^{++}$  tetraquark but they expected the  $X(4274)$  peak to be  $0^{-+}$  in the same model. Molecular interpretations [12–16] found that the  $X(4140)$  can only be a  $J^{PC} = 0^{++}$  or  $2^{++}$   $D_s^{*+}D_s^{*-}$  molecule. Compact tetraquark models expected  $0^{-+}$ ,  $1^{-+}$  [17], or  $0^{++}$ ,  $2^{++}$  [18] state(s) in the mass region of interest. Finally, no evidence of a  $1^{++}$  tetraquark state has been found in a lattice-regularised QCD computation with diquark operators [19].

A similar situation can be found for the  $J^{PC} = 0^{++}$   $X(4500)$  and  $X(4700)$  resonances discovered in the high  $J/\psi\phi$  mass region. For instance, the work of Wang *et al.* [20] predicted only one virtual  $D_s^{*+}D_s^{*-}$  state at  $4.48 \pm 0.17$  GeV. Therefore, the novelty of these states resides in the fact that it is difficult to explain their

\* pgortega@ific.uv.es

† jorge.segovia@tum.de

‡ entem@usal.es

§ fdz@usal.es

structure as molecules or tetraquarks.<sup>1</sup>

In this situation, we first have to remember that coupled-channel effects can generate signals which mimic resonances. These structures may appear near two-particle thresholds if the attraction between the two particles in the channel is not sufficient to produce a resonance but the amplitude behaves as it would be a resonance (cusp) [22]. The near coincidence of the  $D_s^\pm D_s^{*\pm}$  and  $J/\psi\phi$  mass thresholds provides suitable conditions to form cusps. An extensive study of the possible rescattering effects which may contribute to the process  $B^+ \rightarrow J/\psi\phi K^+$  has been performed in, for instance, Ref. [23].

One should also not forget that, in general, a meson can be composed of multi-quark Fock components as  $|M\rangle = |q\bar{q}\rangle + |qq\bar{q}\bar{q}\rangle + \dots$  but the dominant Fock space component is the  $q\bar{q}$  one and thus pure (or dominant) higher excited quark-antiquark states predicted by the naive quark model can appear in the experimental measurements when exploring the higher energy spectrum.

In this work we shall show that the  $X(4140)$  can be interpreted as a cusp in the  $J/\psi\phi$  channel due to the presence of the  $D_s D_s^*$  threshold, whereas the rest of states observed by the LHCb Collaboration in the  $J/\psi\phi$  invariant mass correspond to quark-antiquark structures whose mass is slightly renormalized by the presence of nearby meson-meson thresholds.

We use the constituent quark model (CQM) presented in [24] and updated in [25] (see Refs. [26] and [27] for reviews). The CQM is based on the assumption that the light-quark constituent mass appears owing to the dynamical breaking of chiral symmetry in QCD at some momentum scale. Regardless of the breaking mechanism, the simplest Lagrangian which describes this situation must contain chiral fields to compensate the mass term and can be expressed as [28]

$$\mathcal{L} = \bar{\psi}(i\not{\partial} - M(q^2)U^{\gamma_5})\psi, \quad (1)$$

where  $U^{\gamma_5} = \exp(i\pi^a \lambda^a \gamma_5 / f_\pi)$ ,  $\pi^a$  denotes nine pseudoscalar fields ( $\eta_0, \vec{\pi}, K_i, \eta_8$ ) with  $i = 1, \dots, 4$  and  $M(q^2)$  is the constituent mass. This constituent quark mass, which vanishes at large momenta and is frozen at low momenta at a value around 350 MeV, can be explicitly obtained from the underlying theory but its theoretical point wise behaviour is simulated herein by parameterizing  $M(q^2) = m_q F(q^2)$  with  $m_q$  the bare quark mass and

$$F(q^2) = \left[ \frac{\Lambda^2}{\Lambda^2 + q^2} \right]^{\frac{1}{2}}, \quad (2)$$

<sup>1</sup> It is fair to mention that the  $X(4274)$  meson appears as a natural quark-gluon hybrid candidate since the lowest spin-multiplet predicted by Lattice QCD [21] has an average mass of  $4281 \pm 16$  MeV. However, the quantum numbers of the  $X(4274)$  has been established to be  $1^{++}$  and so this state cannot belong to that multiplet but to the higher one with an average mass of  $4383 \pm 30$  MeV.

where the cut-off  $\Lambda$  fixes the chiral symmetry breaking scale.

The matrix of Goldstone-boson fields can be expanded in the following form

$$U^{\gamma_5} = 1 + \frac{i}{f_\pi} \gamma^5 \lambda^a \pi^a - \frac{1}{2f_\pi^2} \pi^a \pi^a + \dots \quad (3)$$

The first term of the expansion generates the constituent quark mass while the second gives rise to a one-boson exchange interaction between quarks. The main contribution of the third term comes from the two-pion exchange interaction which has been simulated by means of a scalar exchange potential.

In the heavy quark sector chiral symmetry is explicitly broken and we do not need to introduce additional fields. However, the chiral fields introduced above provide a natural way to incorporate the pion-exchange interaction in the molecular dynamics.

The next ingredient of our quark model is the non-relativistic limit of one-gluon exchange (OGE) interaction, the Breit-Fermi interaction, in analogy to positronium. The OGE potential is generated from the vertex Lagrangian [29]

$$\mathcal{L}_{qqg} = i\sqrt{4\pi\alpha_s} \bar{\psi} \gamma_\mu G_c^\mu \lambda^c \psi, \quad (4)$$

where  $\lambda^c$  are the  $SU(3)$  colour matrices,  $G_c^\mu$  is the gluon field and  $\alpha_s$  is the strong coupling constant. The scale dependence of  $\alpha_s$  can be found in *e.g.* Ref. [24], it allows a consistent description of light, strange and heavy mesons.

The last main feature of our constituent quark model is based on the empirical fact that quarks and gluons have never been seen as isolated particles. Colour confinement should be encoded in the non-Abelian character of QCD, however, at present, it is still infeasible to analytically derive these property from the QCD Lagrangian. Lattice-regularised QCD studies have demonstrated that multi-gluon exchanges produce an attractive linearly rising potential proportional to the distance between infinite-heavy quarks [30]. However, the spontaneous creation of light-quark pairs from the QCD vacuum may give rise at the same scale to a breakup of the colour flux-tube [30]. We have tried to mimic these two phenomenological observations by the expression:

$$V_{\text{CON}}(\vec{r}) = [-a_c(1 - e^{-\mu_c r}) + \Delta] (\vec{\lambda}_q^c \cdot \vec{\lambda}_{\bar{q}}^c), \quad (5)$$

where  $a_c$  and  $\mu_c$  are model parameters. At short distances this potential presents a linear behaviour with an effective confinement strength, while at large distances it shows a threshold from which no quark-antiquark bound states can be found. This form of the confining potential, slightly different from the usual one which grows linearly until infinity, is important to describe the higher excited states in the quarkonium spectrum, in particular, the charmonium one.

Explicit expressions for all the potentials and the value of the model parameters can be found in Ref. [24], updated in Ref. [25].

| State       | $J^{PC}$ | $nL$ | Theory (MeV) | Experiment (MeV)          |
|-------------|----------|------|--------------|---------------------------|
| $\chi_{c0}$ | $0^{++}$ | $3P$ | 4241.7       |                           |
|             |          | $4P$ | 4497.2       | $4506 \pm 11_{-15}^{+12}$ |
|             |          | $5P$ | 4697.6       | $4704 \pm 10_{-24}^{+14}$ |
| $\chi_{c1}$ | $1^{++}$ | $3P$ | 4271.5       | $4273.3 \pm 8.3$          |
|             |          | $4P$ | 4520.8       |                           |
|             |          | $5P$ | 4716.4       |                           |

TABLE I. Naive quark-antiquark spectrum in the region of interest of the LHCb [4, 5] for the  $0^{++}$  and  $1^{++}$  channels.

In order to find the quark-antiquark bound states with this constituent quark model, we solve the Schrödinger equation using the Gaussian expansion method [31] (GEM), expanding the radial wave function in terms of basis functions

$$R_\alpha(r) = \sum_{n=1}^{n_{max}} c_n^\alpha \phi_{nl}^G(r), \quad (6)$$

where  $\alpha$  refers to the channel quantum numbers and  $\phi_{nl}^G(r)$  are Gaussian trial functions with ranges in geometric progression. This choice is useful for optimizing the ranges with a small number of free parameters [31]. In addition, the geometric progression is dense at short distances, so that it enables the description of the dynamics mediated by short range potentials.

The coefficients,  $c_n^\alpha$ , and the eigenvalue,  $E$ , are determined from the Rayleigh-Ritz variational principle

$$\sum_{n=1}^{n_{max}} \left[ (T_{n'n}^\alpha - EN_{n'n}^\alpha) c_n^\alpha + \sum_{\alpha'} V_{n'n}^{\alpha\alpha'} c_n^{\alpha'} = 0 \right], \quad (7)$$

where  $T_{n'n}^\alpha$ ,  $N_{n'n}^\alpha$  and  $V_{n'n}^{\alpha\alpha'}$  are the matrix elements of the kinetic energy, the normalization and the potential, respectively.  $T_{n'n}^\alpha$  and  $N_{n'n}^\alpha$  are diagonal, whereas the mixing between different channels is given by  $V_{n'n}^{\alpha\alpha'}$ .

Table I shows the calculated naive quark-antiquark spectrum in the region of interest of the LHCb for the  $J^{PC} = 0^{++}$  and  $1^{++}$  channels. A tentative assignment of the theoretical states with the experimentally observed mesons at the LHCb experiment is also given. It can be seen that the naive quark model is able to reproduce all the new LHCb resonances except the  $X(4140)$ . The  $X(4274)$ ,  $X(4500)$  and  $X(4700)$  appear as conventional charmonium states with quantum numbers  $3^3P_1$ ,  $4^3P_0$  and  $5^3P_0$ , respectively.

Tables II, III and IV show, respectively, the partial and total decay widths of the  $X(4274)$ ,  $X(4500)$  and  $X(4700)$  mesons assuming the above assignment of their quantum numbers. The decay widths have been computed using a modified version of the  $^3P_0$  decay model presented in Ref. [32]. In such a version, the strength  $\gamma$  of the decay interaction depends on the mass scale as

$$\gamma(\mu) = \frac{\gamma_0}{\log\left(\frac{\mu}{\mu_0}\right)}, \quad (8)$$

| State                  | $nL$  | Channel      | $\Gamma$ (MeV) | $\mathcal{B}$ (%) |
|------------------------|-------|--------------|----------------|-------------------|
| $\chi_{c1}$            | $3P$  | $DD$         | —              | —                 |
|                        |       | $DD^*$       | 17.35          | 58.24             |
|                        |       | $DD_0^*$     | 0.26           | 0.88              |
|                        |       | $D^*D^*$     | 0.43           | 1.44              |
|                        |       | $D_sD_s$     | —              | —                 |
|                        |       | $D_sD_s^*$   | 8.49           | 28.48             |
|                        |       | $D_s^*D_s^*$ | 3.26           | 1.95              |
| $56 \pm 11_{-11}^{+8}$ | Total | 29.8         | 100.00         |                   |

TABLE II. Open-flavour strong decay widths, in MeV, and branching fractions, in %, of the  $X(4274)$  meson with quantum numbers  $nJ^{PC} = 31^{++}$ . The experimental value of the total decay width is taken from Ref. [4, 5].

where  $\mu$  is the reduced mass of the quark-antiquark in the decaying meson and,  $\gamma_0 = 0.81 \pm 0.02$  and  $\mu_0 = (49.84 \pm 2.58)$  MeV are parameters determined by the global fit. The value of the  $\gamma$  in the charmonium sector is 0.282.

The total decay width of  $X(4274)$  as the  $3^3P_1$  state is lower than the experimental measurement performed by LHCb [4, 5]. It is worth to mention that the  $X(4274)$  has been measured by the CDF [6] and CMS [8] Collaborations obtaining similar masses than the one of the LHCb but lower values of its total decay width:  $32_{-15}^{+22} \pm 8$  and  $38_{-15}^{+30} \pm 16$ , respectively. These central values are in agreement with our theoretical prediction; in any case, the LHCb determination is fairly compatible with our figure. The information of the partial decay widths shown in Table II points out that the  $DD^*$  and  $D_sD_s^*$  decay channels are dominant with branching ratios of  $\sim 60\%$  and  $\sim 30\%$ , respectively.

One can see in Tables III and IV that the predicted total decay widths for the  $X(4500)$  and  $X(4700)$  mesons as  $J^{PC} = 0^{++}$   $4P$  and  $5P$  states are, within errors, in good agreement with the LHCb observations. Table III shows that the  $DD$ ,  $DD_1^{(\prime)}$ ,  $D^*D_1'$  and  $D^*D_2^*$  decay channels are the most important for the  $X(4500)$  meson with branching fractions ranging between 10% and 25%. Table IV shows that the  $X(4700)$  decays around 50% of the times into  $D^*D_2^*$  final state. Traces in many other channels are found with partial decay widths of several MeV, the most important ones are its decays into  $DD$  and  $D^*D_1'$  final states.

To gain some insight into the nature of the  $X(4140)$ , that does not appear as quark-antiquark state, and to see how the coupling with the open-flavour thresholds can modify the properties of the naive quark-antiquark states predicted above, we have performed a coupled-channel calculation including the  $D^*D_1^{(\prime)}$ ,  $D_sD_s$ ,  $D_s^*D_s^*$  and  $J/\psi\phi$  channels for the  $J^{PC} = 0^{++}$  sector; and the  $D_sD_s^*$ ,  $D_s^*D_s^*$  and  $J/\psi\phi$  ones for the  $J^{PC} = 1^{++}$  sector. These are the allowed channels whose thresholds are in the region studied by the LHCb. It is important to

| State                   | $nL$  | Channel                               | $\Gamma$ (MeV) | $\mathcal{B}$ (%) |
|-------------------------|-------|---------------------------------------|----------------|-------------------|
| $\chi_{c0}$             | 4P    | DD                                    | 13.27          | 11.53             |
|                         |       | DD*                                   | –              | –                 |
|                         |       | DD <sub>0</sub> *                     | –              | –                 |
|                         |       | DD <sub>1</sub>                       | 19.50          | 16.94             |
|                         |       | DD <sub>1</sub> '                     | 27.23          | 23.65             |
|                         |       | DD <sub>2</sub> *                     | –              | –                 |
|                         |       | D*D*                                  | 2.19           | 1.90              |
|                         |       | D*D <sub>0</sub> *                    | 0.86           | 0.75              |
|                         |       | D*D <sub>1</sub>                      | 3.18           | 2.76              |
|                         |       | D*D <sub>1</sub> '                    | 25.86          | 22.47             |
|                         |       | D*D <sub>2</sub> *                    | 18.12          | 15.74             |
|                         |       | D <sub>s</sub> D <sub>s</sub>         | 0.06           | 0.05              |
|                         |       | D <sub>s</sub> D <sub>s</sub> *       | –              | –                 |
|                         |       | D <sub>s</sub> D <sub>s0</sub> *      | –              | –                 |
|                         |       | D <sub>s</sub> D <sub>s1</sub> (2460) | 0.74           | 0.64              |
|                         |       | D <sub>s</sub> D <sub>s</sub> *       | 3.76           | 3.27              |
|                         |       | D <sub>s</sub> D <sub>s0</sub> *      | 0.33           | 0.29              |
| $92 \pm 21^{+21}_{-20}$ | Total | 115.11                                | 100.00         |                   |

TABLE III. Open-flavour strong decay widths, in MeV, and branching fractions, in %, of the  $X(4500)$  meson with quantum numbers  $nJ^{PC} = 40^{++}$ . The experimental value of the total decay width is taken from Ref. [4, 5].

remark here that, in principle, one should couple with the infinite number of meson-meson thresholds but it has been argued by many theorists [33, 34] that the only relevant thresholds are those close to the naive states having the rest a little effect which can be absorbed in our quark model parameters.

Therefore, we assume now that the hadronic state can be described as

$$|\Psi\rangle = \sum_{\alpha} c_{\alpha} |\psi_{\alpha}\rangle + \sum_{\beta} \chi_{\beta}(P) |\phi_A \phi_B \beta\rangle, \quad (9)$$

where  $|\psi_{\alpha}\rangle$  are  $c\bar{c}$  eigenstates solution of the two-body problem,  $\phi_A$  and  $\phi_B$  are the two meson states with  $\beta$  quantum numbers, and  $\chi_{\beta}(P)$  is the relative wave function between the two mesons.

Two- and four-quark configurations are coupled using the same transition operator that has allowed us to compute the above open-flavour strong decays. This is because the coupling between the quark-antiquark and meson-meson sectors requires also the creation of a light quark pair [35, 36]. We define the transition potential  $h_{\beta\alpha}(P)$  within the  ${}^3P_0$  model as [37]

$$\langle \phi_A \phi_B \beta | T | \psi_{\alpha} \rangle = P h_{\beta\alpha}(P) \delta^{(3)}(\vec{P}_{\text{cm}}), \quad (10)$$

where  $P$  denotes the relative momentum of the two-meson state.

Using Eq. (9) and the transition potential in Eq. (10),

| State                             | $nL$  | Channel                               | $\Gamma$ (MeV) | $\mathcal{B}$ (%) |
|-----------------------------------|-------|---------------------------------------|----------------|-------------------|
| $\chi_{c0}$                       | 5P    | DD                                    | 12.32          | 10.10             |
|                                   |       | DD*                                   | –              | –                 |
|                                   |       | DD <sub>0</sub> *                     | –              | –                 |
|                                   |       | DD <sub>1</sub>                       | 6.93           | 5.68              |
|                                   |       | DD <sub>1</sub> '                     | 3.61           | 2.96              |
|                                   |       | DD <sub>2</sub> *                     | –              | –                 |
|                                   |       | D*D*                                  | 8.77           | 7.19              |
|                                   |       | D*D <sub>0</sub> *                    | 5.69           | 4.66              |
|                                   |       | D*D <sub>1</sub>                      | 2.32           | 1.90              |
|                                   |       | D*D <sub>1</sub> '                    | 20.39          | 16.71             |
|                                   |       | D*D <sub>2</sub> *                    | 56.22          | 46.07             |
|                                   |       | D <sub>s</sub> D <sub>s</sub>         | 0.11           | 0.09              |
|                                   |       | D <sub>s</sub> D <sub>s</sub> *       | –              | –                 |
|                                   |       | D <sub>s</sub> D <sub>s0</sub> *      | –              | –                 |
|                                   |       | D <sub>s</sub> D <sub>s1</sub> (2460) | 2.41           | 1.98              |
|                                   |       | D <sub>s</sub> D <sub>s1</sub> (2536) | 0.26           | 0.22              |
|                                   |       | D <sub>s</sub> D <sub>s2</sub> *      | –              | –                 |
|                                   |       | D <sub>s</sub> D <sub>s</sub> *       | 1.36           | 1.12              |
|                                   |       | D <sub>s</sub> D <sub>s0</sub> *      | 1.27           | 1.04              |
|                                   |       | D <sub>s</sub> D <sub>s1</sub> (2460) | 0.29           | 0.24              |
|                                   |       | D <sub>s</sub> D <sub>s1</sub> (2536) | 0.00           | 0.00              |
| D <sub>s</sub> D <sub>s2</sub> *  | 0.03  | 0.02                                  |                |                   |
| D <sub>s0</sub> D <sub>s0</sub> * | 0.03  | 0.03                                  |                |                   |
| $120 \pm 30^{+42}_{-33}$          | Total | 122.02                                | 100.00         |                   |

TABLE IV. Open-flavour strong decay widths, in MeV, and branching fractions, in %, of the  $X(4700)$  meson with quantum numbers  $nJ^{PC} = 50^{++}$ . The experimental value of the total decay width is taken from Ref. [4, 5].

we arrive to the coupled equations

$$c_{\alpha} M_{\alpha} + \sum_{\beta} \int h_{\alpha\beta}(P) \chi_{\beta}(P) P^2 dP = E c_{\alpha}, \quad (11)$$

$$\sum_{\beta} \int H_{\beta'\beta}(P', P) \chi_{\beta}(P) P^2 dP + \sum_{\alpha} h_{\beta'\alpha}(P') c_{\alpha} = E \chi_{\beta'}(P'), \quad (12)$$

where  $M_{\alpha}$  are the masses of the bare  $c\bar{c}$  mesons and  $H_{\beta'\beta}$  is the resonant group method (RGM) Hamiltonian for the two-meson states obtained from the  $q\bar{q}$  interaction.

Solving the coupled-channel equations, Eqs. (11) and (12), as indicated in, e.g., Ref. [38], we obtain the results shown in Tables V and VI for the  $J^{PC} = 0^{++}$  channel and in Tables VII and VIII for the  $J^{PC} = 1^{++}$  channel.

Table V shows that we obtain two states with  $J^{PC} = 0^{++}$  quantum numbers made by a  $\sim 50\%$  of  $c\bar{c}$  component and by a similar amount of molecular components. Their masses are close to those associated with the bare  $q\bar{q}$   $J^{PC} = 0^{++}$  4P and 5P states. Table VI shows that the

| Mass   | Width | $\mathcal{P}_{c\bar{c}}$ | $\mathcal{P}_{D^*D_1}$ | $\mathcal{P}_{D^*D'_1}$ | $\mathcal{P}_{D_sD_s}$ | $\mathcal{P}_{D_s^*D_s^*}$ | $\mathcal{P}_{J/\psi\phi}$ |
|--------|-------|--------------------------|------------------------|-------------------------|------------------------|----------------------------|----------------------------|
| 4493.6 | 79.2  | 57.2                     | 8.4                    | 33.1                    | 0.9                    | 0.4                        | < 0.1                      |
| 4674.1 | 50.2  | 47.6                     | 27.2                   | 21.0                    | 1.6                    | 2.6                        | < 0.1                      |

TABLE V. Mass, in MeV, total decay width, in MeV, and probability of each Fock component, in %, for the  $X(4500)$  and  $X(4700)$  mesons. The calculated widths include both the contributions of the  $c\bar{c}$  and molecular components. The results have been calculated in the coupled-channel quark model.

| Mass (MeV) | $\mathcal{P}_{c\bar{c}}$ | $\mathcal{P}_{(n<3)P}$ | $\mathcal{P}_{3P}$ | $\mathcal{P}_{4P}$ | $\mathcal{P}_{5P}$ | $\mathcal{P}_{(n>5)P}$ |
|------------|--------------------------|------------------------|--------------------|--------------------|--------------------|------------------------|
| 4493.6     | 57.2                     | 3.033                  | 11.332             | 80.037             | 5.573              | 0.026                  |
| 4674.1     | 47.6                     | 0.014                  | 0.001              | 2.062              | 97.071             | 0.853                  |

TABLE VI. Probabilities, in %, of  $nP$   $c\bar{c}$  bare states for the  $X(4500)$  and  $X(4700)$  mesons.

| Mass   | Width | $\mathcal{P}_{c\bar{c}}$ | $\mathcal{P}_{D_sD_s^*}$ | $\mathcal{P}_{D_s^*D_s^*}$ | $\mathcal{P}_{J/\psi\phi}$ |
|--------|-------|--------------------------|--------------------------|----------------------------|----------------------------|
| 4242.4 | 25.9  | 48.7                     | 43.5                     | 5.0                        | 2.7                        |

TABLE VII. Mass, in MeV, total decay width, in MeV, and probability of each Fock component, in %, for the  $X(4274)$  meson. The calculated widths include both the contributions of the  $c\bar{c}$  and molecular components. The results have been calculated in the coupled-channel quark model.

object with a mass of 4493.6 MeV is almost a pure  $4P$   $c\bar{c}$  state whereas the object with a mass of 4674.1 MeV is almost a pure  $5P$   $c\bar{c}$  state. Then, we first conclude that the net effect of coupling the thresholds to both naive quark-antiquark states is to modify the mass of the bare  $c\bar{c}$  states in a modest amount. The second observation is that the total decay widths of these two states are significantly reduced. The new values, 79.2 MeV and 50.2 MeV, are lower than the central ones reported by the LHCb but still within the experimental uncertainty interval.

In the coupled-channel calculation of the  $J^{PC} = 1^{++}$  channel, we include the  $D_sD_s^*$ ,  $D_s^*D_s^*$  and  $J/\psi\phi$  thresholds. We found only one state with mass 4242.4 MeV and total decay width 25.9 MeV. This state is made by 48.7% of the  $3P$  charmonium state and by 43.5% of the  $D_sD_s^*$  component (see Tables VII and VIII). When coupling with thresholds, the modification in the mass and width is small. Our total decay width is still compatible with the LHCb result, but indicates that the lower CDF and CMS measurements are in better agreement with our prediction. We again show in Table VIII that the dominant charmonium component of such physical state is the  $3P$   $c\bar{c}$  one.

As we do not find any signal for the  $X(4140)$ , neither bound nor virtual, we analyze the line shape of the  $J/\psi\phi$  channel as an attempt to explain the  $X(4140)$  as a simple

| Mass (MeV) | $\mathcal{P}_{c\bar{c}}$ | $\mathcal{P}_{1P}$ | $\mathcal{P}_{2P}$ | $\mathcal{P}_{3P}$ | $\mathcal{P}_{4P}$ | $\mathcal{P}_{(n>4)P}$ |
|------------|--------------------------|--------------------|--------------------|--------------------|--------------------|------------------------|
| 4242.4     | 48.7                     | 0.000              | 0.370              | 99.037             | 0.488              | 0.105                  |

TABLE VIII. Probabilities, in %, of  $nP$   $c\bar{c}$  bare states for the  $X(4274)$  meson.

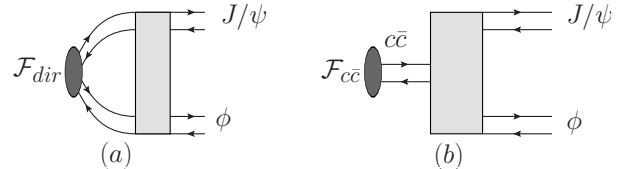


FIG. 1. Diagrams of the two possible production mechanisms for the  $J/\psi\phi$  channel: Direct production through a point-like source (a) or production through intermediate  $c\bar{c}$  states (b).

threshold cusp.

We evaluate the production of  $J/\psi\phi$  pairs via two main mechanisms: (i) the direct generation of  $J/\psi$  and  $\phi$  mesons from a point-like source and (ii) the production via intermediate  $c\bar{c}$  states. Therefore, the line-shape is given by

$$\frac{dB(J/\psi\phi)}{dE} = \mathcal{B} k \left[ |\mathcal{M}_{\text{point}}|^2 + |\mathcal{M}_{c\bar{c}}|^2 \right] \Theta(E), \quad (13)$$

with  $k$  the on-shell momentum. The  $\mathcal{M}_{\text{point}}$  is the direct production of  $J/\psi\phi$  given by (Fig. 1a):

$$\mathcal{M}_{\text{point}}^\beta(E) = \mathcal{F}_{\text{point}} \times \left( 1 - \sum_{\beta'} \int dP T^{\beta\beta'}(E; k, P) \frac{2\mu P^2}{P^2 - k^2} \right)_{\text{on-shell}}, \quad (14)$$

where  $\mathcal{F}_{\text{point}}$  is the production amplitude from a point-like source.

In addition,  $\mathcal{M}_{c\bar{c}}$  is the production via  $c\bar{c}$  states (Fig. 1b), which can be expressed as

$$\mathcal{M}_{c\bar{c}}^\beta = -\mathcal{F}_{c\bar{c}} \sum_{\alpha\alpha'} \Phi_{\alpha'\beta}(E; k) \Delta_{\alpha'\alpha}(E)^{-1}, \quad (15)$$

where  $\mathcal{F}_{c\bar{c}}$  is the production amplitude from a  $c\bar{c}$  state,  $\Phi$  is the  $^3P_0$  vertex dressed by the RGM interaction and  $\Delta$  is the complete propagator (see Ref. [38] for details).

Figure 2 compares our result with that reported by the LHCb Collaboration in the  $B^+ \rightarrow J/\psi\phi K^+$  decays. The rapid increasing observed in the data near the  $J/\psi\phi$  threshold corresponds with a bump in the theoretical result just above such threshold. This cusp is too wide to be produced by a bound or virtual state below the  $J/\psi\phi$  threshold. If one fixes, attending to the experimental data, the normalization  $\mathcal{B}$  in Eq. (13) to each contribution separately, one realizes that the

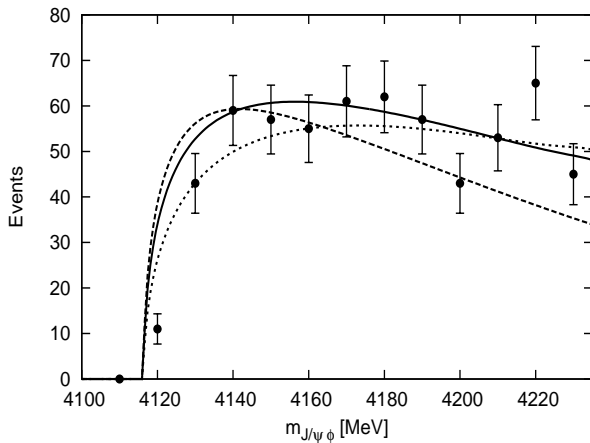


FIG. 2. Line-shape prediction of the  $J/\psi\phi$  channel. The solid curve is the result of Eq. (13). The other two curves show the production of  $J/\psi\phi$  pairs via two main mechanisms: the direct generation of  $J/\psi$  and  $\phi$  mesons from a point-like source (dotted curve) and the production via intermediate  $c\bar{c}$  states (dashed curve). Note that the normalization  $\mathcal{B}$  in Eq. (13) has been fitted to the data for each curve.

production via intermediate  $c\bar{c}$  states is dominant at low values of the invariant mass, which is reasonable as the point-like production should be suppressed because the number of particles to be created is twice; whereas, at high energies, it is the direct generation of  $J/\psi$  and  $\phi$  mesons from a point-like source which drives the production.

As a summary, we have analysed in a coupled-channel quark model the  $J/\psi\phi$  structures reported by the LHCb Collaboration in the amplitude analysis of the  $B^+ \rightarrow J/\psi\phi K^+$  decays. Three of them, namely  $X(4274)$ ,  $X(4500)$  and  $X(4700)$  are consistent with bare quark-antiquark states with quantum numbers, respectively,  $J^{PC} = 1^{++}(3P)$ ,  $J^{PC} = 0^{++}(4P)$  and  $J^{PC} = 0^{++}(5P)$ . The agreement between theory and experiment is due in part by our particular choice of the confining potential: screened-linear. Partial and total decay widths of the  $X(4274)$ ,  $X(4500)$  and  $X(4700)$  mesons have been also

computed using a version of the  $^3P_0$  decay model in which its only parameter has been constrained before in other meson sectors. The coupling of the naive quark-antiquark states with the near meson-meson thresholds modifies slightly their properties but does not generate new resonances.

In the  $1^{++}$  sector we do not find any pole in the mass region of the  $X(4140)$ . However, the scattering amplitude shows a bump just above the  $J/\psi\phi$  threshold which reproduces the rapid increasing of the experimental data. Therefore, the structure showed by this data around 4140 MeV should be interpreted as a cusp due to the presence of the  $D_s D_s^*$  threshold. The residual  $D_s - D_s^*$  interaction is too weak to develop a bound or virtual state.

The experimental results constitute a prominent example of the interplay between quark and meson degrees of freedom in near open-flavoured threshold regions. Depending on the dynamics of the system, the presence of these thresholds can generate new states, simply renormalizes the masses of the bare  $q\bar{q}$  states or produces cusp effects at threshold when the interactions are not strong enough to produce bound states.

Finally, these results also reinforce the validity of the constituent quark model to qualitatively describe the phenomenology of the excited heavy quark meson states and get insights on the dynamics that leads their formation.

## ACKNOWLEDGMENTS

This work has been partially funded by Ministerio de Ciencia y Tecnología under Contract no. FPA2013-47443-C2-2-P, by the Spanish Excellence Network on Hadronic Physics FIS2014-57026-REDT, and by the Junta de Castilla y León under Contract no. SA041U16. P. G. Ortega acknowledges the financial support of the Spanish Ministerio de Economía y Competitividad and European FEDER funds under the contracts FIS2014-51948-C2-1-P. J. Segovia acknowledges the financial support from Alexander von Humboldt Foundation.

- 
- [1] M. Gell-Mann, Phys. Lett. **8**, 214 (1964).
  - [2] G. Zweig, CERN Report No.8182/TH.401, CERN Report No.8419/TH.412 (1964).
  - [3] K. A. Olive *et al.* (Particle Data Group), Chin. Phys. **C38**, 090001 (2014).
  - [4] R. Aaij *et al.* (LHCb), (2016), arXiv:1606.07895 [hep-ex].
  - [5] R. Aaij *et al.* (LHCb), (2016), arXiv:1606.07898 [hep-ex].
  - [6] T. Aaltonen *et al.* (CDF), ArXiv:hep-ex/1101.6058.
  - [7] V. M. Abazov *et al.* (D0), Phys. Rev. Lett. **115**, 232001 (2015).
  - [8] S. Chatrchyan *et al.* (CMS), Phys. Lett. **B734**, 261 (2014).
  - [9] C. P. Shen *et al.* (Belle), Phys. Rev. Lett. **104**, 112004 (2010).
  - [10] J. P. Lees *et al.* (BaBar), Phys. Rev. **D91**, 012003 (2015).
  - [11] R. F. Lebed and A. D. Polosa, Phys. Rev. **D93**, 094024 (2016).
  - [12] X. Liu and S.-L. Zhu, Phys. Rev. **D80**, 017502 (2009), [Erratum: Phys. Rev. D85, 019902 (2012)].
  - [13] T. Branz, T. Gutsche, and V. E. Lyubovitskij, Phys. Rev. **D80**, 054019 (2009).
  - [14] R. M. Albuquerque, M. E. Bracco, and M. Nielsen, Phys. Lett. **B678**, 186 (2009).

- [15] G.-J. Ding, Eur. Phys. J. **C64**, 297 (2009).
- [16] J.-R. Zhang and M.-Q. Huang, J. Phys. **G37**, 025005 (2010).
- [17] N. V. Drenska, R. Faccini, and A. D. Polosa, Phys. Rev. **D79**, 077502 (2009).
- [18] Z.-g. Wang and Y.-f. Tian, Int. J. Mod. Phys. **A30**, 1550004 (2015).
- [19] M. Padmanath, C. B. Lang, and S. Prelovsek, Phys. Rev. **D92**, 034501 (2015).
- [20] Z.-G. Wang, Z.-C. Liu, and X.-H. Zhang, Eur. Phys. J. **C64**, 373 (2009).
- [21] L. Liu, G. Moir, M. Peardon, S. M. Ryan, C. E. Thomas, P. Vilaseca, J. J. Dudek, R. G. Edwards, B. Joo, and D. G. Richards (Hadron Spectrum), JHEP **07**, 126 (2012).
- [22] D. V. Bugg, in *Proceedings, 10th International Workshop on Meson Production, Properties and Interaction (MESON 2008)*, arXiv:hep-ph/0806.3566.
- [23] X.-H. Liu, (2016), arXiv:hep-ph/1607.01385.
- [24] J. Vijande, F. Fernandez, and A. Valcarce, J. Phys. **G31**, 481 (2005).
- [25] J. Segovia, A. Yasser, D. R. Entem, and F. Fernandez, Phys. Rev. **D78**, 114033 (2008).
- [26] A. Valcarce, H. Garcilazo, F. Fernandez, and P. Gonzalez, Rept. Prog. Phys. **68**, 965 (2005).
- [27] J. Segovia, D. R. Entem, F. Fernandez, and E. Hernandez, Int. J. Mod. Phys. **E22**, 1330026 (2013).
- [28] D. Diakonov, Prog. Part. Nucl. Phys. **51**, 173 (2003).
- [29] A. De Rujula, H. Georgi, and S. L. Glashow, Phys. Rev. **D12**, 147 (1975).
- [30] G. S. Bali, H. Neff, T. Duessel, T. Lippert, and K. Schilling (SESAM), Phys. Rev. **D71**, 114513 (2005).
- [31] E. Hiyama, Y. Kino, and M. Kamimura, Prog. Part. Nucl. Phys. **51**, 223 (2003).
- [32] J. Segovia, D. R. Entem, and F. Fernandez, Phys. Lett. **B715**, 322 (2012), arXiv:1205.2215 [hep-ph].
- [33] E. S. Swanson, J. Phys. **G31**, 845 (2005).
- [34] T. Barnes and E. S. Swanson, Phys. Rev. **C77**, 055206 (2008).
- [35] A. Le Yaouanc, L. Oliver, O. Pene, and J. Raynal, Phys. Rev. **D8**, 2223 (1973).
- [36] A. Le Yaouanc, L. Oliver, O. Pene, and J.-C. Raynal, Phys. Rev. **D9**, 1415 (1974).
- [37] Y. Kalashnikova, Phys. Rev. **D72**, 034010 (2005).
- [38] P. G. Ortega, D. R. Entem, and F. Fernandez, J. Phys. **G40**, 065107 (2013).